

Supporting Information

Controlled Synthesis and Enhanced Gas Sensing Performance of Zinc-Doped Indium Oxide Nanowires

Che-Wen Yu ¹, Hsuan-Wei Fu ¹, Shu-Meng Yang ¹, Yu-Shan Lin ¹ and Kuo-Chang Lu ^{1,2*}

¹ Department of Materials Science and Engineering, National Cheng Kung University, Tainan 701, Taiwan; n56091352@gs.ncku.edu.tw (C.-W.Y.); n56091556@gs.ncku.edu.tw (H.-W.F.); n56074287@gs.ncku.edu.tw (S.-M.Y.); n56114053@gs.ncku.edu.tw (Y.-S.L.)

² Core Facility Center, National Cheng Kung University, Tainan 701, Taiwan

* Correspondence: gkclu@mail.ncku.edu.tw; Tel.: +886-6-275-7575 (ext. 62920)

List of contents

Figure S1 | Schematic illustration of the growth mechanism of Zn-In₂O₃ nanowires. The reaction followed the VLS route(a)~(c).

Figure S2 | SEM image of zinc clusters on indium oxide nanowires.

Figure S3 | Composition analysis of(a) In₂O₃ nanowire (b) 3 at% Zn-In₂O₃ nanowire (c) 5 at% Zn-In₂O₃ nanowire.

Figure S4 | The mapping images of(a) In₂O₃ nanowire (b) 3 at% Zn-In₂O₃ nanowire (c) 5 at% Zn-In₂O₃ nanowire.

Figure S5 | (a,b) SEM images of single In₂O₃ nanowire-based electrical measurement micro-device. I-V measurements of single In₂O₃ nanowire. (c) R₁₃₊ (d) R₁₃₋ (e) R₁₄₊ (f) R₁₄₋ (g) R₂₃₊ (h) R₂₃₋ (i) R₂₄₊ (j) R₂₄₋.

Figure S6 | (a,b) SEM image of single 3 at% Zn-In₂O₃ nanowire-based electrical measurement micro-device. I-V measurements of 3 at% Zn-In₂O₃ nanowire. (c) R₁₃₊ (d) R₁₃₋ (e) R₁₄₊ (f) R₁₄₋ (g) R₂₃₊ (h) R₂₃₋ (i) R₂₄₊ (j) R₂₄₋.

Figure S7 | (a,b) SEM image of single 5 at% Zn-In₂O₃ nanowire-based electrical measurement micro-device. I-V measurements of 5 at% Zn-In₂O₃ nanowire. (c) R₁₃₊ (d) R₁₃₋ (e) R₁₄₊ (f) R₁₄₋ (g) R₂₃₊ (h) R₂₃₋ (i) R₂₄₊ (j) R₂₄₋.

Figure S8 | (a-d) Dynamic gas sensing curves of single In₂O₃ nanowire, 3 at% Zn-In₂O₃ nanowire and 5 at% Zn-In₂O₃ nanowire at 150 °C, 200 °C, 250 °C and 300 °C to 5 ppm acetone.

Figure S9 | (a-d) Dynamic gas sensing curves of single In₂O₃ nanowire, 3 at% Zn-In₂O₃ nanowire and 5 at% Zn-In₂O₃ nanowire at 150 °C, 200 °C, 250 °C, and 300 °C to 5 ppm carbon monoxide.

Figure S10 | (a-d) Dynamic gas sensing curves of single In₂O₃ nanowire, 3 at% Zn-In₂O₃ nanowire and 5 at% Zn-In₂O₃ nanowire at 150 °C, 200 °C, 250 °C and 300 °C to 5 ppm ethanol.

Figure S11 | Schematic illustration of the change of electron depletion region after n-type semiconductor absorbs reducing gas.

Table S1 | Summary of gas sensing performance of In₂O₃, 3 at% Zn-In₂O₃, 5 at% Zn-In₂O₃ nanowires.

Table S2 | Comparison with previous sensing studies on In₂O₃ nanowires with different dopants for

5ppm ethanol.

Table S3 | Comparison with previous sensing studies on In_2O_3 nanostructures with different dopants for 5ppm acetone.

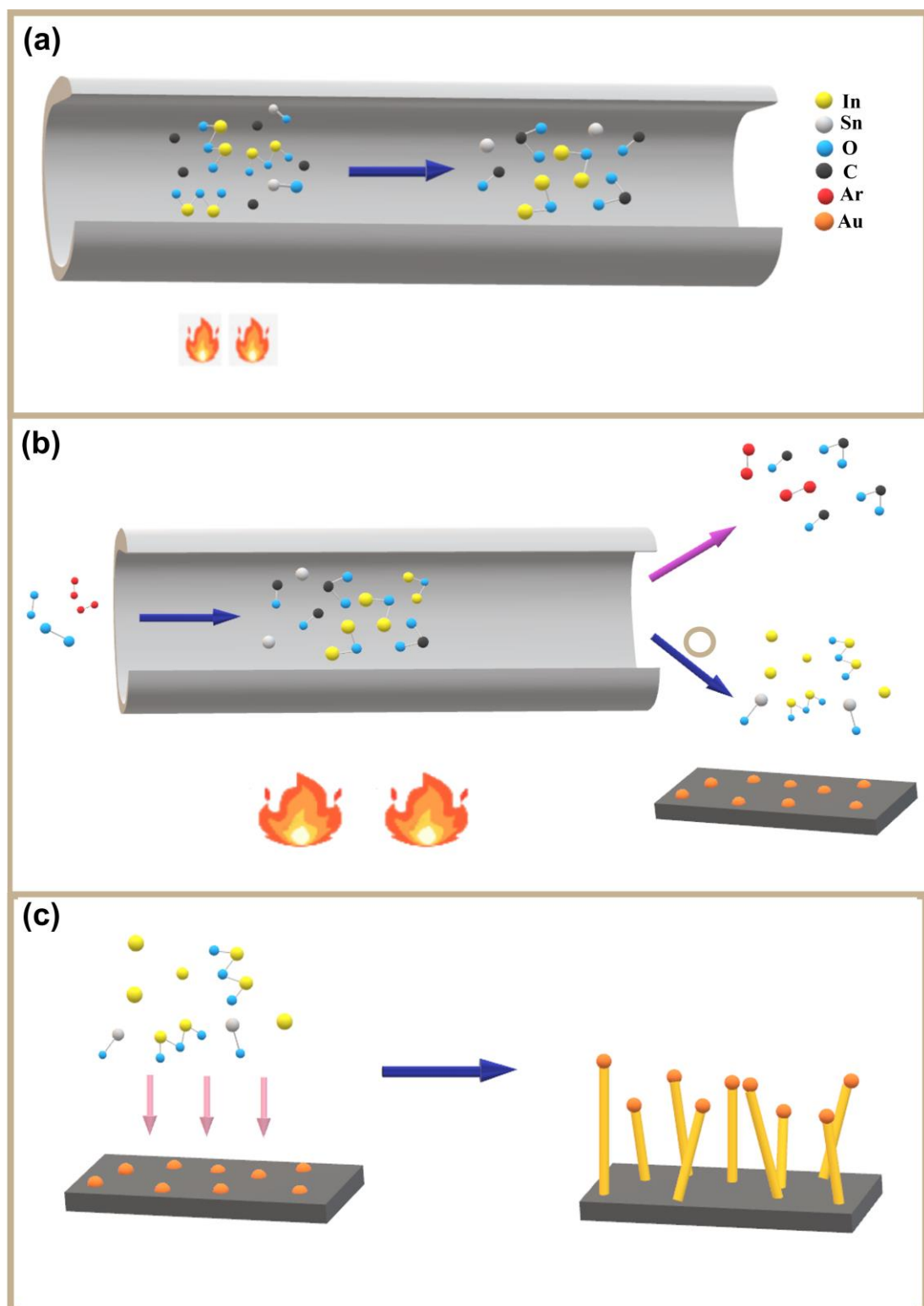


Figure S1 Schematic illustration of the growth mechanism of Zn-In₂O₃ nanowires.
The reaction followed the VLS route(a)~(c).

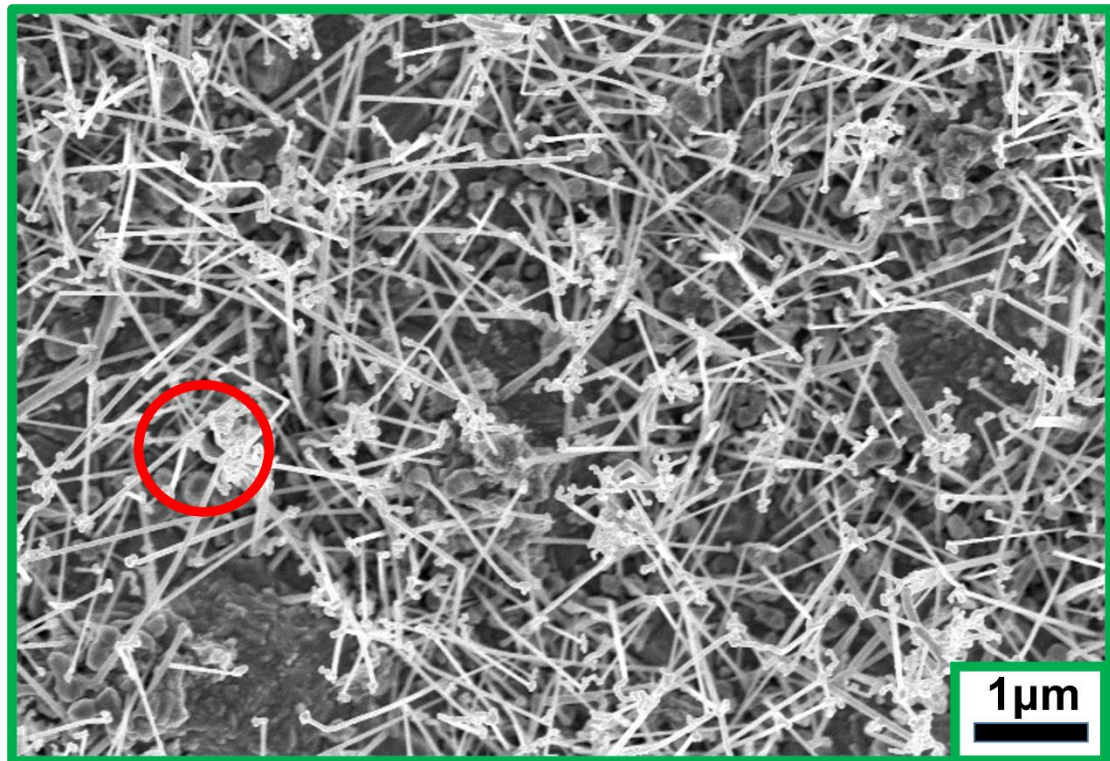


Figure S2 SEM image of zinc clusters on indium oxide nanowires.

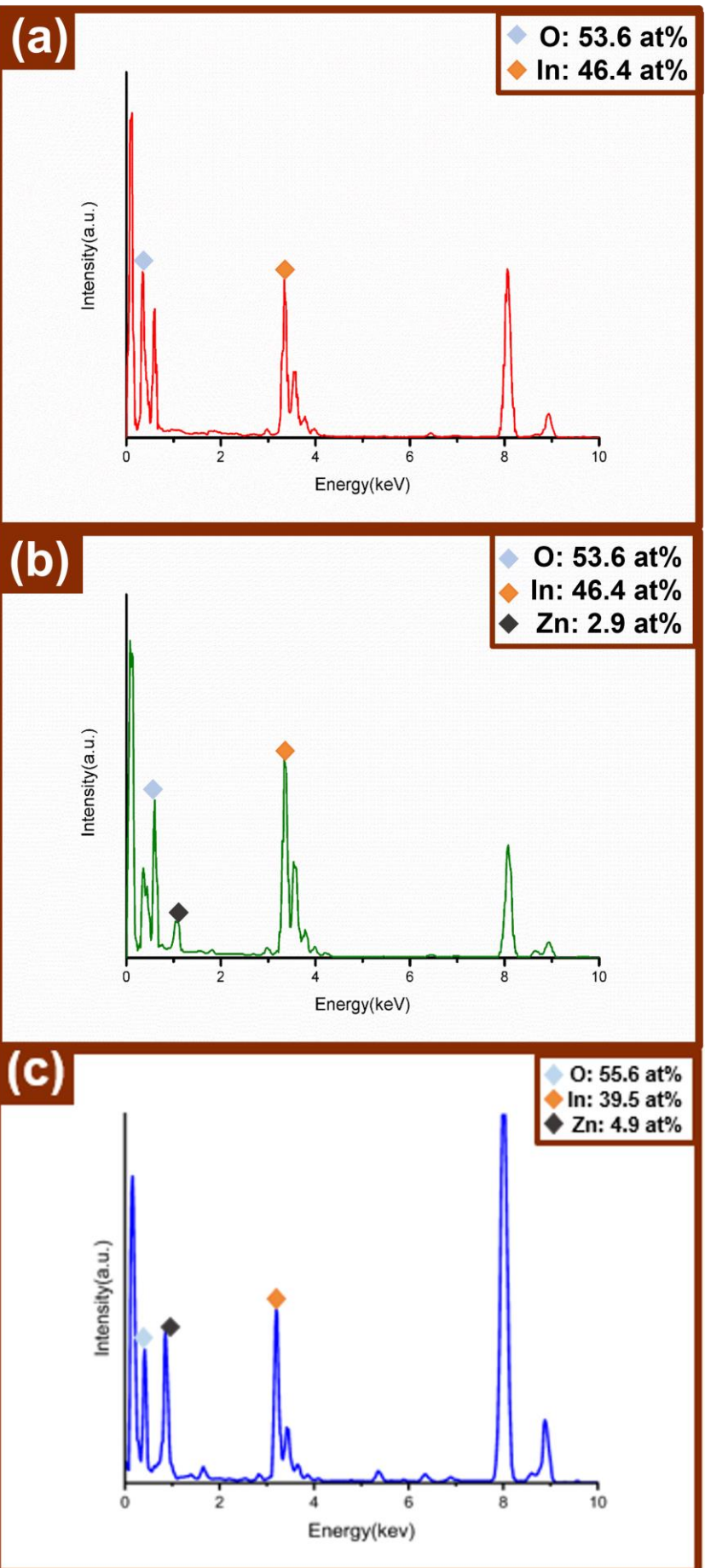


Figure S3 Composition analysis of(a) In_2O_3 nanowire (b) 3 at% Zn- In_2O_3 nanowire (c) 5 at% Zn- In_2O_3 nanowire.

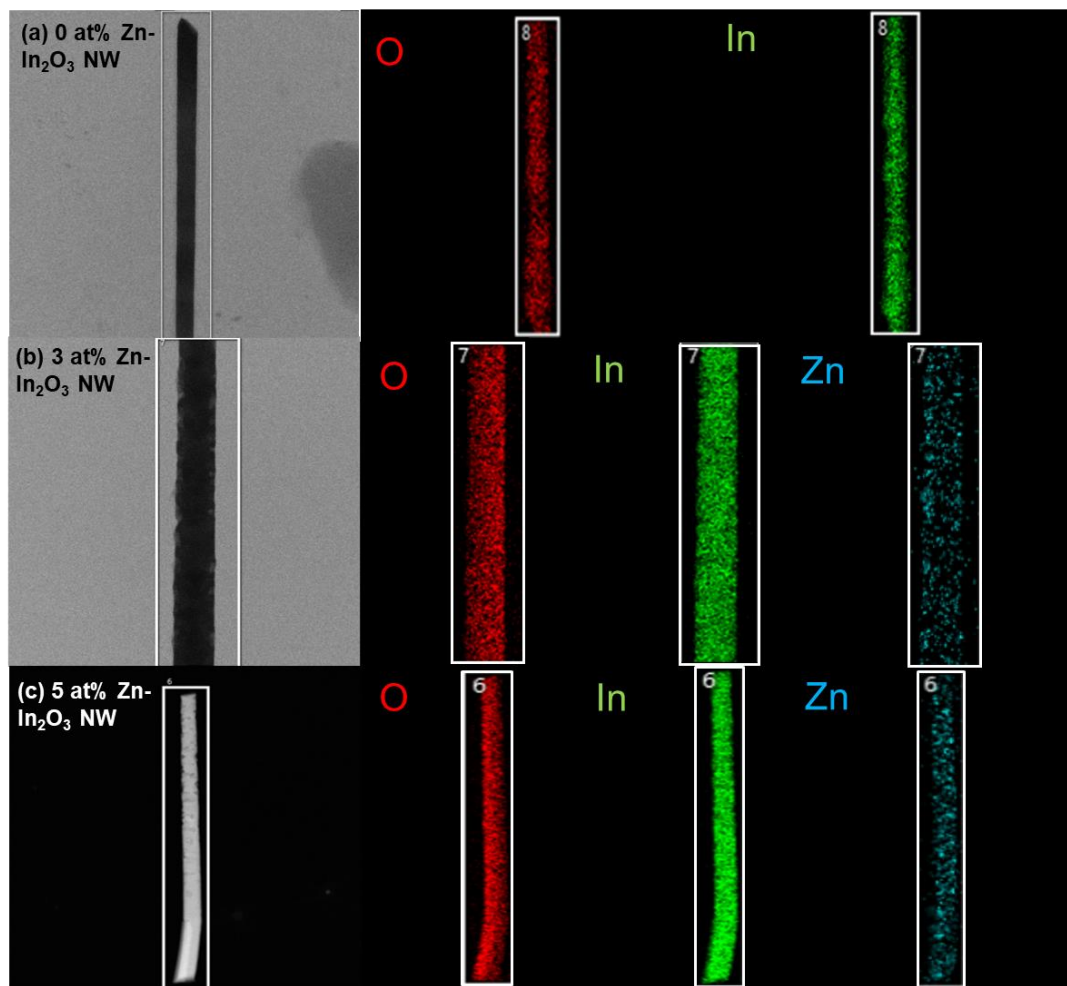


Figure S4 The mapping images of(a) In_2O_3 nanowire (b) 3 at% Zn- In_2O_3 nanowire (c) 5 at% Zn- In_2O_3 nanowire.

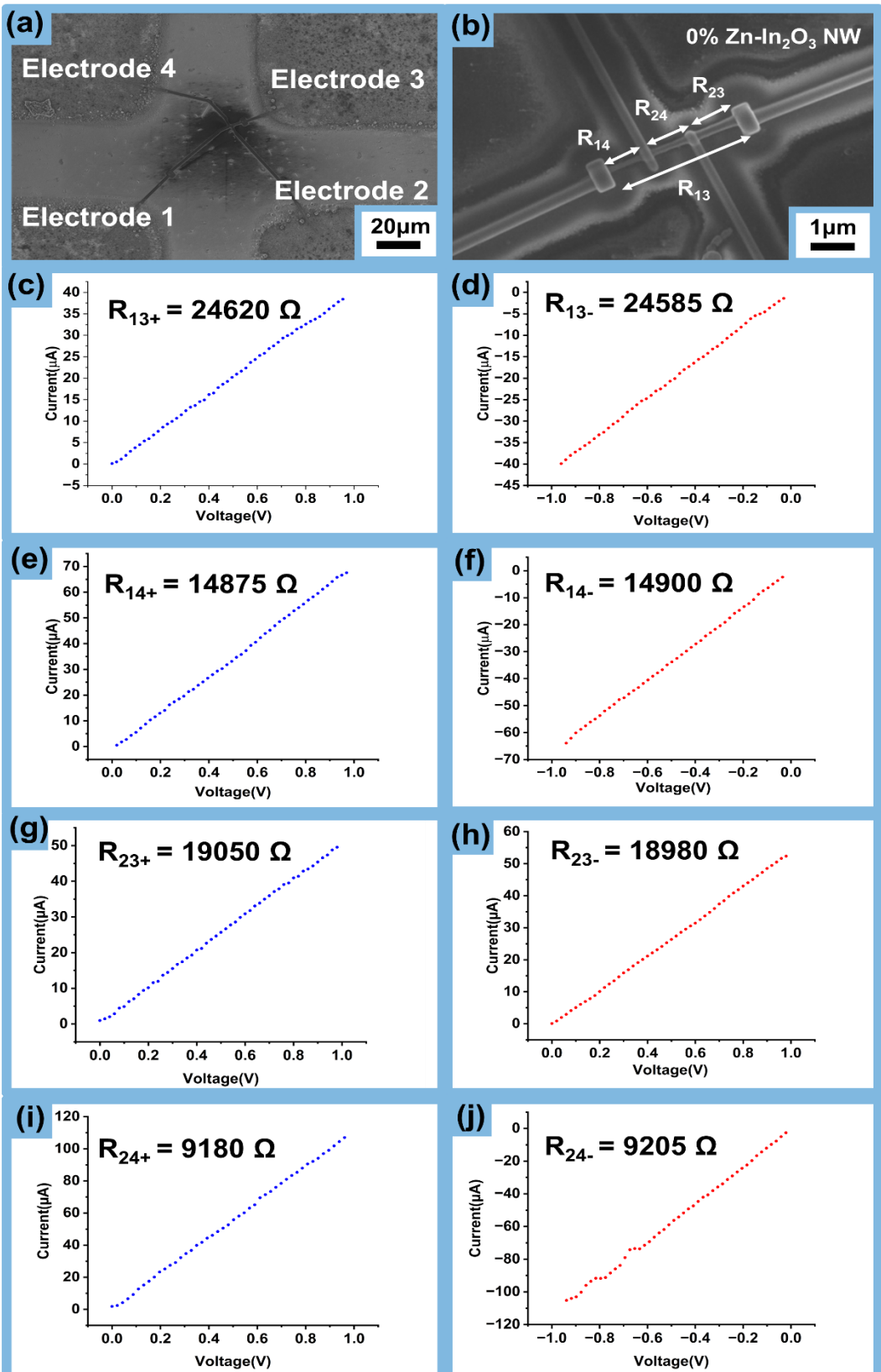


Figure S5. (a,b) SEM images of single In₂O₃ nanowire-based electrical measurement micro-device. I-V measurements of single In₂O₃ nanowire. (c) R₁₃₊ (d) R₁₃₋ (e) R₁₄₊ (f) R₁₄₋ (g) R₂₃₊ (h) R₂₃₋ (i) R₂₄₊ (j) R₂₄₋.

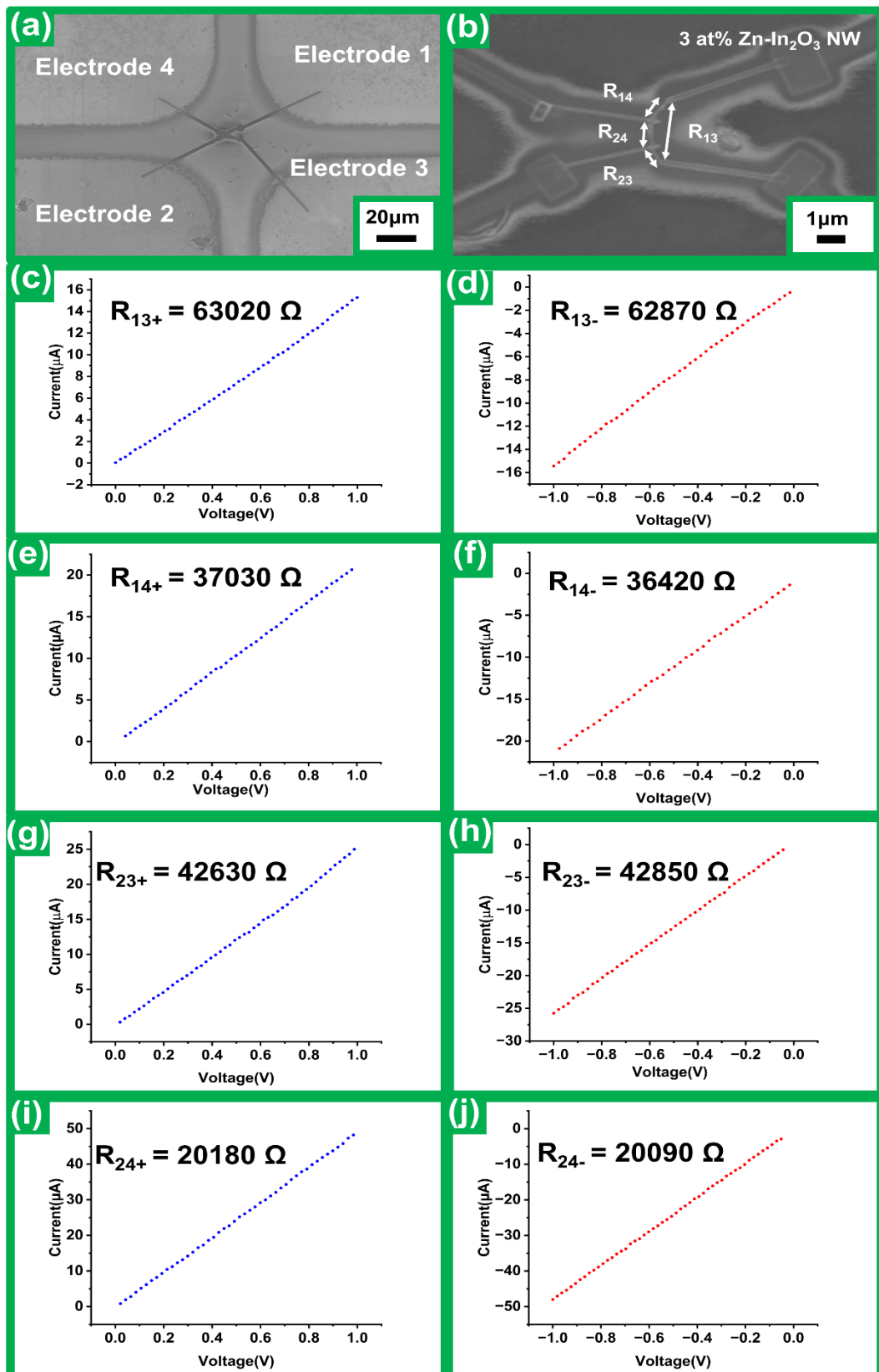


Figure S6. (a,b) SEM image of single 3 at% Zn-In₂O₃ nanowire-based electrical measurement micro-device. I-V measurements of 3 at% Zn- In₂O₃ nanowire. (c) R₁₃₊ (d) R₁₃₋ (e) R₁₄₊ (f) R₁₄₋ (g) R₂₃₊ (h) R₂₃₋ (i) R₂₄₊ (j) R₂₄₋.

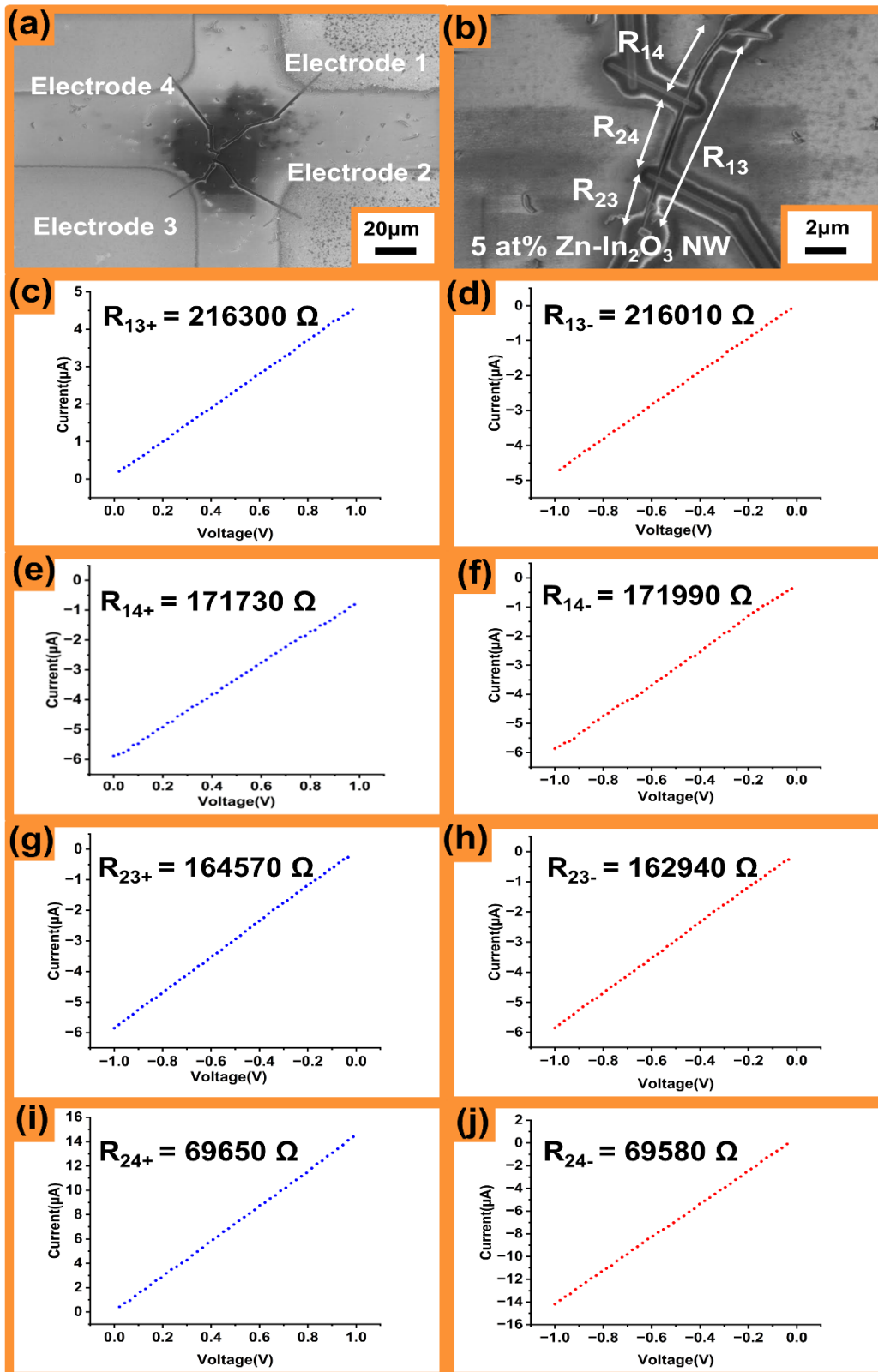


Figure S7. (a,b) SEM image of single 5 at% Zn-In₂O₃ nanowire-based electrical measurement micro-device. I-V measurements of 5 at% Zn-In₂O₃ nanowire. (c) R₁₃₊ (d) R₁₃₋ (e) R₁₄₊ (f) R₁₄₋ (g) R₂₃₊ (h) R₂₃₋ (i) R₂₄₊ (j) R₂₄₋.

5 ppm acetone

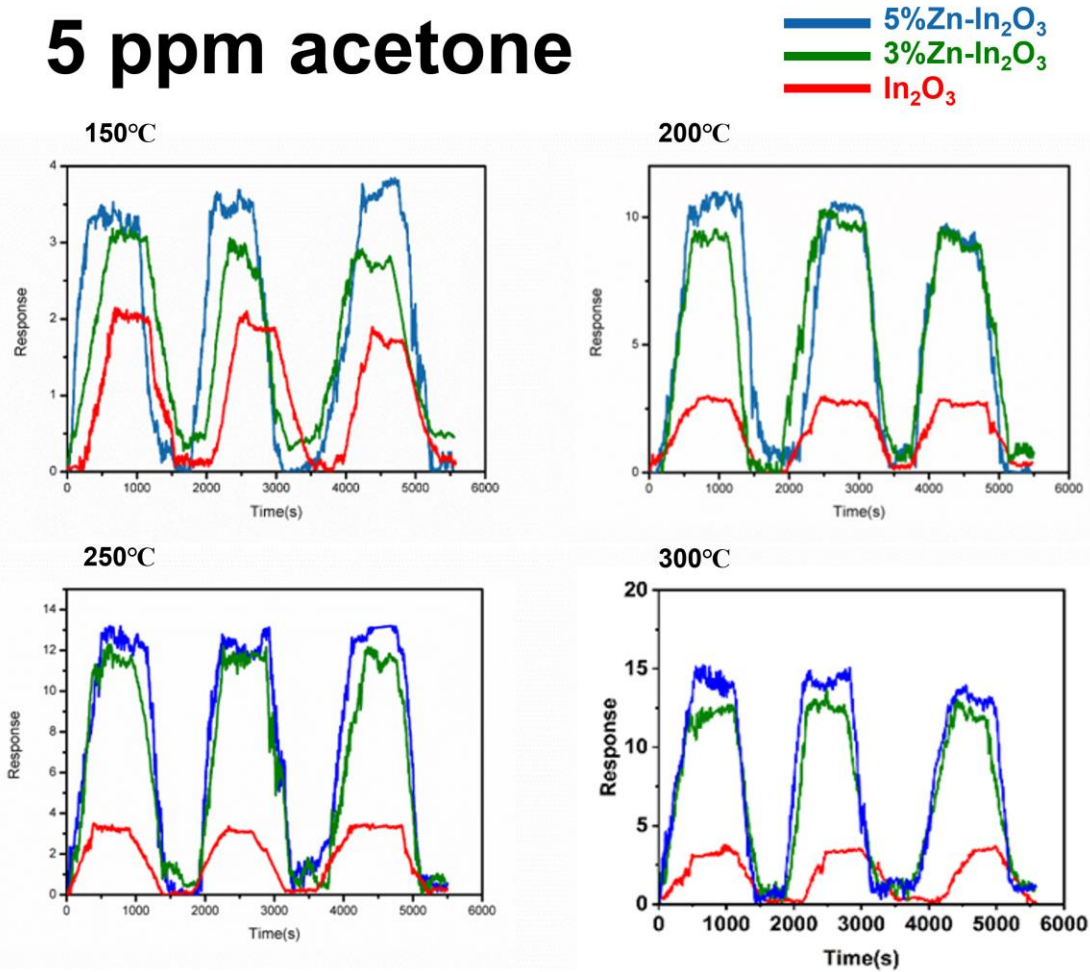


Figure S8. (a-d) Dynamic gas sensing curves of single In₂O₃ nanowire, 3 at% Zn-In₂O₃ nanowire and 5 at% Zn-In₂O₃ nanowire at 150 °C, 200 °C, 250 °C and 300 °C to 5 ppm acetone.

5 ppm carbon monoxide

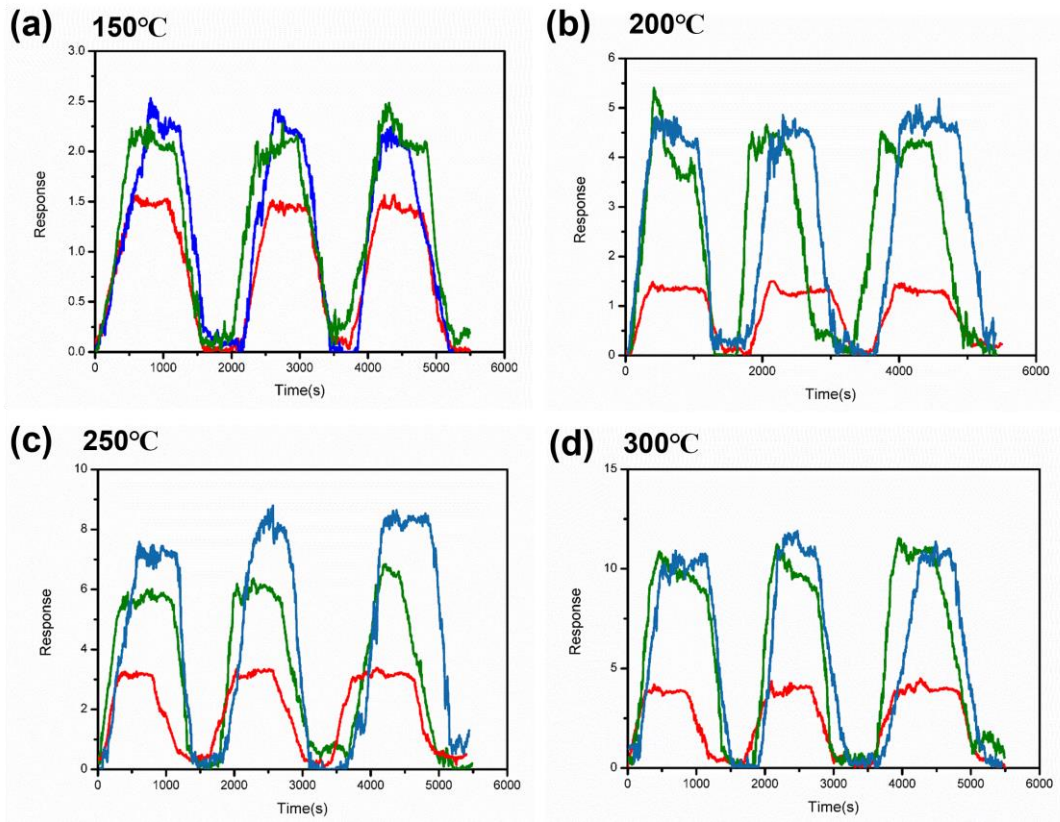
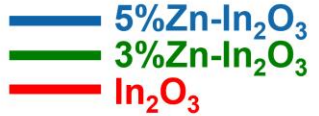


Figure S9. (a-d) Dynamic gas sensing curves of single In₂O₃ nanowire, 3 at% Zn-In₂O₃ nanowire and 5 at% Zn-In₂O₃ nanowire at 150 °C, 200 °C, 250 °C, and 300 °C to 5 ppm carbon monoxide.

5 ppm ethanol

— 5%Zn-In₂O₃
— 3%Zn-In₂O₃
— In₂O₃

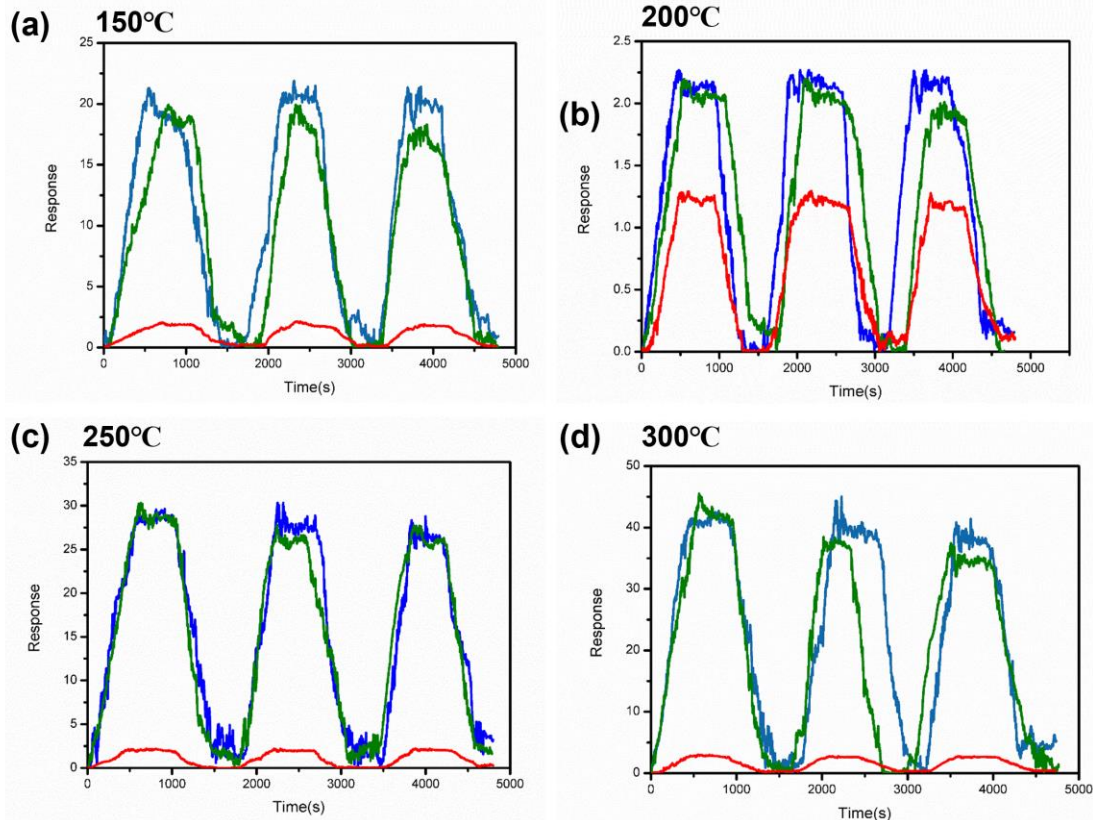


Figure S10. (a-d) Dynamic gas sensing curves of single In₂O₃ nanowire, 3 at% Zn-In₂O₃ nanowire and 5 at% Zn-In₂O₃ nanowire at 150 °C, 200 °C, 250 °C and 300 °C to 5 ppm ethanol.

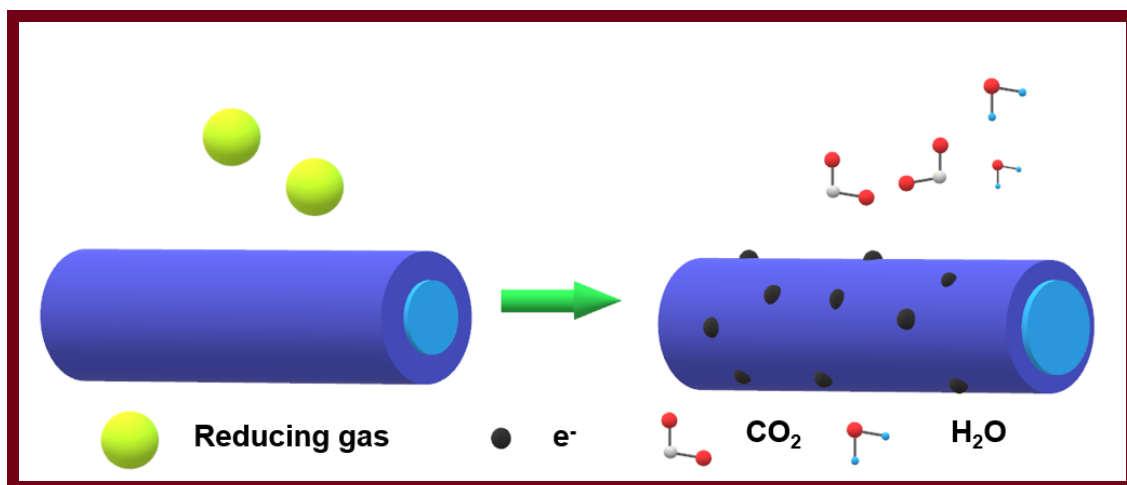


Figure S11. Schematic illustration of the change of electron depletion region after n-type semiconductor absorbs reducing gas.

Table S1. Summary of gas sensing performance of In_2O_3 , 3 at% Zn-In₂O₃, 5 at% Zn-In₂O₃ nanowires.

Acetone	150°C	200°C	250°C	300°C
In_2O_3	2.0	2.9	3.5	3.4
3% Zn-In ₂ O ₃	2.8	9.9	12.1	12.3
5% Zn-In ₂ O ₃	3.5	10.9	13.2	13.9
Carbon monoxide	150°C	200°C	250°C	300°C
In_2O_3	1.5	1.2	3.2	3.8
3% Zn-In ₂ O ₃	2.2	3.8	6.1	10.0
5% Zn-In ₂ O ₃	2.3	4.5	7.2	10.8
Ethanol	150°C	200°C	250°C	300°C
In_2O_3	1.3	1.8	2.2	2.5
3% Zn-In ₂ O ₃	2.2	18.1	30.7	36.8
5% Zn-In ₂ O ₃	2.3	20.1	29.7	40.7

Table S2. Comparison with previous sensing studies on In₂O₃ nanowires with different dopants for 5ppm ethanol.

Sensing element	Gas concentration	Temperature	Response	Reference
In ₂ O ₃ NW	5ppm	300°C	2.5	This work
3% Zn-doped In ₂ O ₃ NW	5ppm	300°C	36.8	This work
5% Zn-doped In ₂ O ₃ NW	5ppm	300°C	40.7	This work
In ₂ O ₃ NWs	20ppm	300°C	30	[5]
5% Sn-doped In ₂ O ₃ NWs	10ppm	400°C	5	[22]
0.5% Co-doped In ₂ O ₃ NWs	100ppm	300°C	16	[23]

Table S3. Comparison with previous sensing studies on In₂O₃ nanostructures with different dopants for 5ppm acetone.

Sensing element	Gas concentration	Temperature	Response	Reference
In ₂ O ₃ NW	5ppm	300°C	3.4	This work
3% Zn-doped In ₂ O ₃ NW	5ppm	300°C	12.3	This work
5% Zn-doped In ₂ O ₃ NW	5ppm	300°C	13.9	This work
Electrospinning In ₂ O ₃ NWs	10ppm	200°C	10	[24]
3% Ag-doped In ₂ O ₃ NPs	50ppm	300°C	7	[25]
0.5% Co-doped In ₂ O ₃ NPs	5ppm	240°C	4	[26]